



Preparation and Mechanical Properties of Graphene Reinforced Poly(vinyl alcohol) Nanocomposites

CHUNYAN WANG, HONGFU WU and YONG QIAN*

Fundamental Science on Radioactive Geology and Exploration Technology Laboratory, Department of Materials Science and Engineering, East China Institute of Technology, Nanchang 330013, Jiangxi Province, P.R. China

*Corresponding author: Tel/Fax: +86 791 83897912; E-mail: yqianecit@163.com

Received: 2 June 2014;

Accepted: 19 August 2014;

Published online: 10 January 2015;

AJC-16658

The incorporation of carbon nanomaterials significantly affected the macroscopic properties of the polymer-based composites. In this paper, graphene oxide nanosheets which exhibited excellent dispersibility and compatibility in poly(vinyl alcohol) matrix were successfully incorporated into poly(vinyl alcohol) through solution mixing; the mechanical properties and reinforced mechanism were investigated in detail. A 52.3 % increase in the tensile strength and a 94.2 % improvement in the Young's modulus were achieved for 2 wt. % graphene oxide loading. The success of this method provides a good rationale for developing high-performance poly(vinyl alcohol)-based composite materials.

Keywords: Poly(vinyl alcohol), Graphene oxide, Mechanical properties.

INTRODUCTION

Graphene, a sp^2 -bonded one-atom-thick two-dimensional carbon layer, has been becoming increasingly widespread¹⁻³ due to its fascinating properties such as outstanding mechanical properties^{4,5}, good electrical conductivity⁶, high surface area⁷, impermeability to gases⁸, and low cost. Graphene and its derivatives (graphene/graphite oxide, functionalized graphene, etc.) have been widely studied in various fields including field-effect transistors⁹, lithium ion batteries¹⁰, drug delivery and cell imaging^{11,12}, chemical and biosensor^{13,14}, supercapacitors¹⁵, removal of toxic material¹⁶, solar cells¹⁷, fuel cells¹⁸, catalysts¹⁹, and polymer nanocomposites^{20,21}, etc. Recently, more and more researchers are actively exploring graphene-based polymer composites to achieve those unique properties such as mechanical strength and modulus, thermal stability and electrical conductivity^{20,21}, which depend extraordinarily on the dispersion of the graphene in the polymer matrices. A well-dispersed state makes the reinforced surface area so maximized that it will affect the nearby polymer chains and the properties of the whole matrix. Considering the strong aggregation of pristine graphene sheets (hydrophobic in nature) in various polymer matrices, graphene oxide (GO) is commonly used as the starting material in place of graphene^{22,23}. Hydrophilic nature makes it highly dispersible in aqueous media as individual sheets. In fact, graphene oxide is also a potential nanofiller for polymer composites for its large aspect ratio and high mechanical strength. Furthermore, in view of its abundant

oxygen-containing groups and hydrophilic nature, graphene oxide exhibits a more effective enhancement effect than pristine graphene for polar polymers such as poly(vinyl alcohol), polymethyl methacrylate, polyimide^{21,24,25}. Poly(vinyl alcohol) (PVA) is a polar polymer consisting many of hydroxyl groups in its main chain, which make dispersion easy. Owing to hydrophilic, biocompatible, good membrane-forming and non-toxic properties, poly(vinyl alcohol) is widely used in drug delivery²⁶, fuel cells²⁷, functional membranes²⁸, coating materials, textile sizing and adhesives^{29,30}.

In this work, we present preparation of PVA/GO composite films through solution mixing and thermal reduction. The mechanical properties and the enhanced mechanism of composites were investigated. Moreover, we also demonstrate a favorable method of dispersion that yields nanoscale dispersions of graphene sheets in poly(vinyl alcohol) solution without addition of surfactant.

EXPERIMENTAL

Natural graphite powder (300 mesh), potassium permanganate, sodium nitrate, 98 % sulfuric acid, 30 % hydrogen peroxide and 37 % hydrochloric acid were purchased from China Medicine Co., China. All the reactants were of analytical grade. poly(vinyl alcohol) with repeat unit number of 2500 was purchased from Beijing Chem. Reagents Co. (Beijing, China)

Preparation of GO/PVA nanocomposite films: Graphene oxide was prepared from graphite by the modified Hummers

method in this work as described elsewhere^{31,32}. Well-dispersed GO/PVA nanocomposites were fabricated through a simple solution-mixing method. The synthesis procedure for a typical 2 wt. % GO/PVA was as follows: 9.8 g poly(vinyl alcohol) was dissolved in 100 mL deionized water at 90 °C in a three-neck flask with mechanical stirring to form an aqueous solution. A homogeneous aqueous graphene oxide dispersion (1 mg/mL) was obtained by sonication at room temperature. Then, 200 mL graphene oxide aqueous suspension was dripped into the poly(vinyl alcohol) solution which was then stirred at 90 °C for 24 h. Finally, the blending was cast onto polytetrafluoroethylene plates and kept in vacuum at 60 °C for 48 h to form flat films, which were peeled off and further heated at 80 °C for 48 h to remove residual water. The other composite film with different loadings were similarly process.

Transmission electron microscopy (TEM) images were obtained from JEM-2100 (Japan) with a 200 kV accelerating voltage. The TEM samples were prepared by drying a droplet of the suspensions on a Cu grid. Atomic force micrographs (AFM) were recorded at an Agilent 5500 AFM/SPM system with Picoscan v 5.3.3 software in tapping mode with samples prepared by spin-coating sample solutions onto freshly exfoliated mica substrates at 1000 rpm under ambient conditions. Scanning electron microscopy (SEM) images were taken from FEI NanoSEM at 15 kv, spot 3. The exposed cross-sections

were sputtered with a thin layer of gold (Emitech K100X) to promote conductivity before SEM observation. X-ray photoelectron spectroscopy (XPS, K_{α}) analyses were carried out on a thermo fisher X-ray photoelectron spectrometer system equipped with Al radiation as a probe, with a chamber pressure of 5×10^{-9} torr. The source power was set at 72 W, and pass energies of 200 eV for survey scans and 50 eV for high-resolution scans were used. The analysis spot size was 400 μm in diameter. X-ray diffractions (XRD) were carried out using a D8 advance (Bruker) X-ray diffractometer with Cu K_{α} radiation ($\lambda = 1.5418 \text{ \AA}$). Raman spectra were recorded using a Renishaw *in via* micro-Raman system with an excitation wavelength of 514 nm. The mechanical properties were measured using SANS CMT-8102 stretching tester at a speed of 5 mm/min using thin films of about 5-10 μm thickness. At least five specimens were used for each sample in the tensile test.

RESULTS AND DISCUSSION

Structures and morphologies of graphene oxide:

Graphene oxide, which contains many oxygen-containing functional groups, can be dispersed very well in water at the level of individual sheets³³. The morphologies and thicknesses of graphene oxide nanosheets can be directly observed by AFM. The samples for AFM analysis were prepared by spin-coating the graphene oxide dispersed in dimethyl acetamide

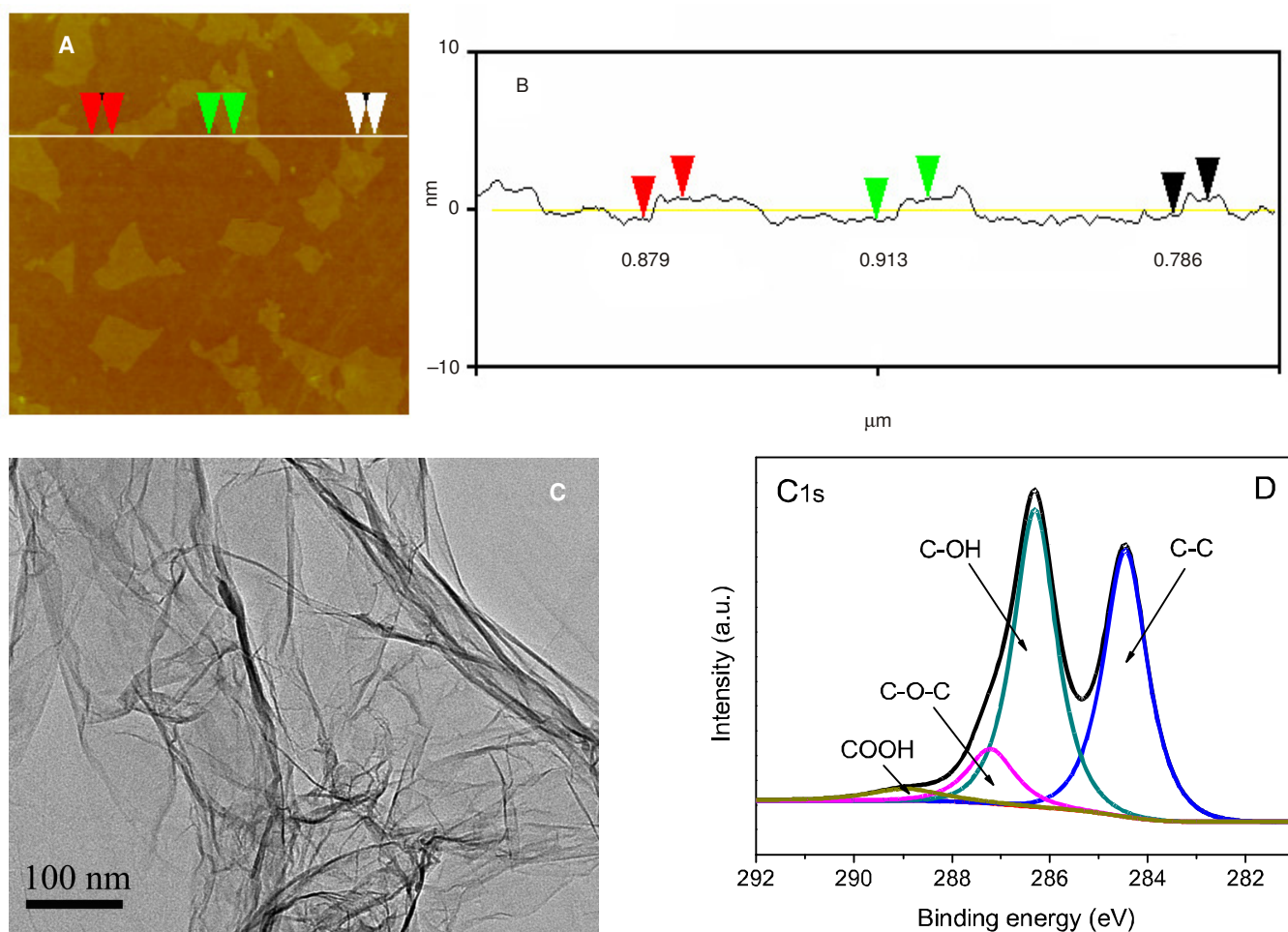


Fig. 1. (A and B) Typical tapping-mode AFM image of graphene oxide deposited on mica substrate from an aqueous dispersion and height profile of (A), (C) TEM image of as-prepared graphene oxide, (D) high-resolution C1s XPS of graphene oxide

onto freshly exfoliated mica and dried at room temperature. Flattened graphene oxide nanosheets without agglomerate appeared as shown in Fig. 1A. The AFM topography image (Fig. 1B) indicates the thickness of the as-prepared graphene oxide to be 0.78–0.92 nm, corresponding to single atomic graphene, as reported previously³². A single-layer pristine graphene is atomically flat with a well-known theoretical thickness of around 0.34 nm. The graphene oxide is expected to be thicker mainly because of the presence of epoxy, hydroxyl and carboxylic acid groups on the surface and edge of the graphene oxide sheets. This unique structural characteristic of graphene oxide sheets can make them strongly hydrophilic and easily disperse in an aprotic solvent. Fig. 1C showed the TEM image of graphene oxide nanosheets, the transparency of the nanosheet suggested a thin thickness of the film. The wrinkles observed were probably caused by the oxygen functionalization and the resultant defects. The TEM images also showed that graphene oxide was fully exfoliated into individual sheets by ultrasonic treatment. X-ray photoelectron spectroscopy (XPS) provides abundant information about the surface composition of graphene oxide. Four typical peaks of graphene oxide centered at 284.5, 286.3, 287.2 and 289 eV as shown in Fig. 1D, corresponding to C=C/C-C (sp^2 and sp^3), C-OH, C-O-C and -COOH groups, respectively.

It is well known that the homogeneous dispersion of nanofillers in the polymer matrix plays a key role in the preparation of high-performance nanocomposites. Fig. 2 shows the photograph of the pure poly(vinyl alcohol) and PVA-GO composite aqueous solution. With the increase of the graphene oxide content, the colour of the composite solution become more and more yellow compared to the colourless pure poly(vinyl alcohol). Moreover, all the GO-PVA composite solution exhibits homogeneous appearance by visual inspection, indicating uniform dispersion of graphene oxide in the poly(vinyl alcohol) matrix. That is, poly(vinyl alcohol) molecular chains are successfully grafted onto the surface of graphene oxide.

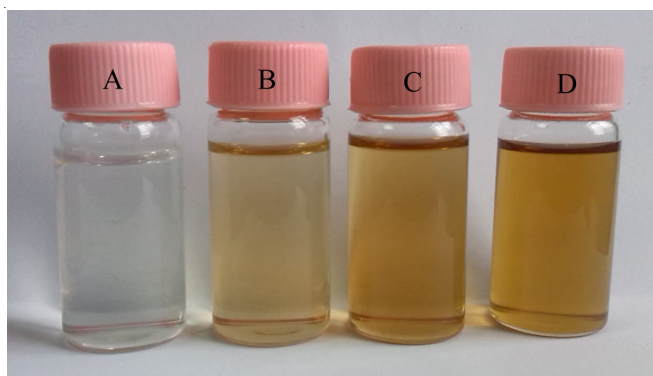


Fig. 2. Photograph of poly(vinyl alcohol), 0.5 % GO/PVA, 1 % GO/PVA and 2 % GO/PVA dispersion in water respectively

Fig. 3 shows the XRD patterns of graphene oxide, pure poly(vinyl alcohol), and 2 % GO/PVA composite films. The typical diffraction peak of graphene oxide was observed at about $2\theta = 10.2^\circ$, corresponding to the layer-to-layer distance of 0.93 nm. This result is consistent with that of AFM. It is significantly larger than that of pristine graphite (0.34 nm),

due to the intercalation of oxygen-containing functional groups³². The XRD patterns of pure poly(vinyl alcohol) film (red curve) and 2 % GO/PVA composite film (blue curve) show characteristic diffraction peaks at $2\theta = 19.6^\circ$. The peak intensity of composite is larger than that of the pure poly(vinyl alcohol). This result indicated that graphene oxide sheets were well exfoliated and homogeneously dispersed at the molecular level in poly(vinyl alcohol) matrix and the crystalline structure of poly(vinyl alcohol) was slightly affected by the incorporation of graphene oxide nanosheets.

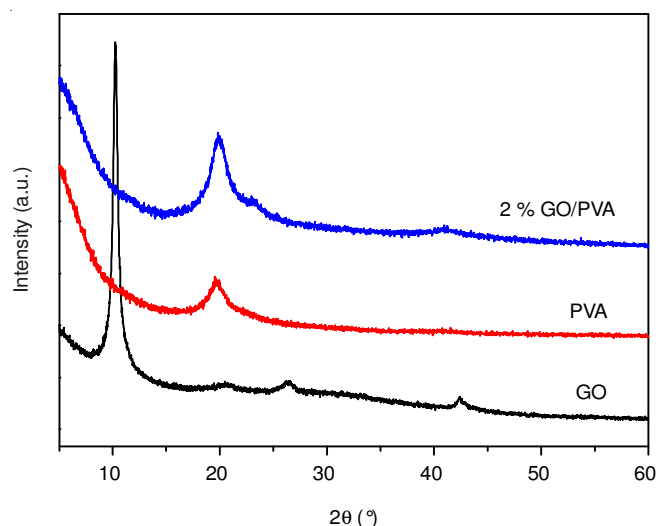


Fig. 3. XRD patterns of graphene oxide, poly(vinyl alcohol) and 2 % GO/PVA composite

Mechanical properties

Inset: magnification of the green section: Pristine graphene is the strongest material with a 130 GPa elastic modulus and 1.1 TPa⁵⁷. Therefore, the effective incorporation of graphene may enhance the mechanical properties of the polymer-based composites. The representative stress-strain curves of pure poly(vinyl alcohol) and PVA/GO films with various amounts of graphene oxide are shown in Fig. 4, and the detailed parameters of mechanical properties are summarized in Table-1. It is obvious that the composites show a higher tensile strength and Young's modulus than those of pure poly(vinyl alcohol). Furthermore, both the tensile strength and modulus of the PVA/GO films increased with increasing graphene oxide component. The tensile strength of the composite containing 2 % of graphene oxide increased by 52.3 % from 55.1 to 83.9 MPa and the Young's improved modulus by 94.2 % compared with the pure poly(vinyl alcohol) film (1.55GPa). The composite contained 2 wt. % graphene oxide film also exhibited a large elongation-at-break ($56.90 \pm 8.1\%$), though this value is smaller than that of pure poly(vinyl alcohol) film ($106.55 \pm 13.9\%$). These results indicated that the composite film is strong and flexible. The significant reinforcement effect of the graphene oxide sheets can be mainly attributed to two aspects: (1) Good compatibility between the graphene oxide sheets and poly(vinyl alcohol) chains. The covalent interactions can prevent their stacking and aggregation and hinder the phase separation. (2) Homogeneous dispersion and strong interaction of the graphene oxide sheets in the

poly(vinyl alcohol) matrix may facilitate the efficient load transfer from the poly(vinyl alcohol) matrix to the nanofillers. Besides, the value of the elongation-at-break decreased compared with neat poly(vinyl alcohol) film. It is because the well-dispersed graphene oxide sheets within the poly(vinyl alcohol) matrix and the strong PVA-GO interfacial interaction hindered the free movement or mobility of the PVA chains during the extension.

TABLE-1
MECHANICAL PROPERTIES OF PURE PVA FILMS
AND PVA/GO-REINFORCED COMPOSITE FILMS
WITH VARIOUS AMOUNTS OF GRAPHENE OXIDE

Sample	Tensile strength (MPa)	Young's modulus (GPa)	Elongation at break (%)
Pure poly(vinyl alcohol) film	55.1 ± 5.15	1.55 ± 0.25	106.55 ± 13.9
0.5 % GO/PVA	69.4 ± 5.41	2.51 ± 0.26	80.03 ± 13.2
1 % GO/PVA	75.6 ± 5.35	2.63 ± 0.23	70.43 ± 12.4
2 % GO/PVA	83.9 ± 5.72	3.01 ± 0.22	56.90 ± 8.1

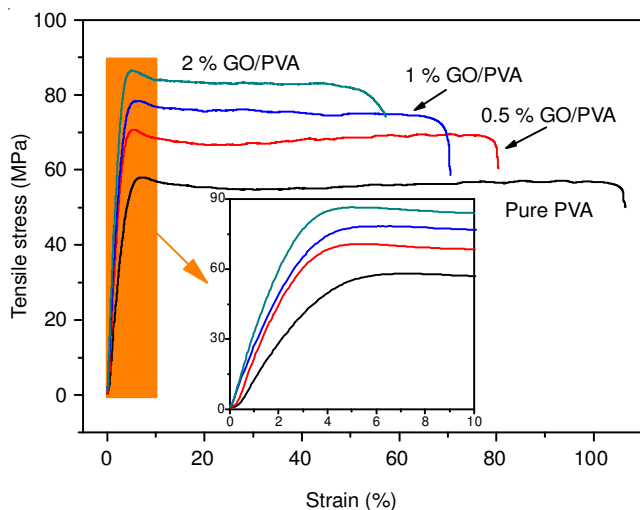


Fig. 4. Typical stress-strain curves of pure PVA and PVA/GO films with various amounts of graphene oxide.

The fracture surfaces of pure poly(vinyl alcohol) and 2 % GO/PVA composite were observed by SEM after tensile testing as shown in Fig. 5. Pure poly(vinyl alcohol) film (Fig. 5A) possesses a smooth and flat fractured surface. For 2 % GO/PVA, the well-dispersed graphene oxide throughout poly(vinyl alcohol) matrix is indicated by the red arrows. The fracture surfaces are comparatively rough compared to neat poly(vinyl alcohol) film as illustrated in Fig. 5B. This can be attributed to the strong interfacial interaction and good compatibility between the graphene oxide sheets and the poly(vinyl alcohol) chains. Such strong interactions are favorable to the stress transfer from the poly(vinyl alcohol) matrix to the graphene sheets, leading to the improvement in the mechanical properties of the composite films compared to those of the pure poly(vinyl alcohol) films.

Conclusion

In summary, we reported a facile method for the successful preparation of high-performance GO/PVA composites by solution mixing. graphene oxide nanosheets exhibited excellent

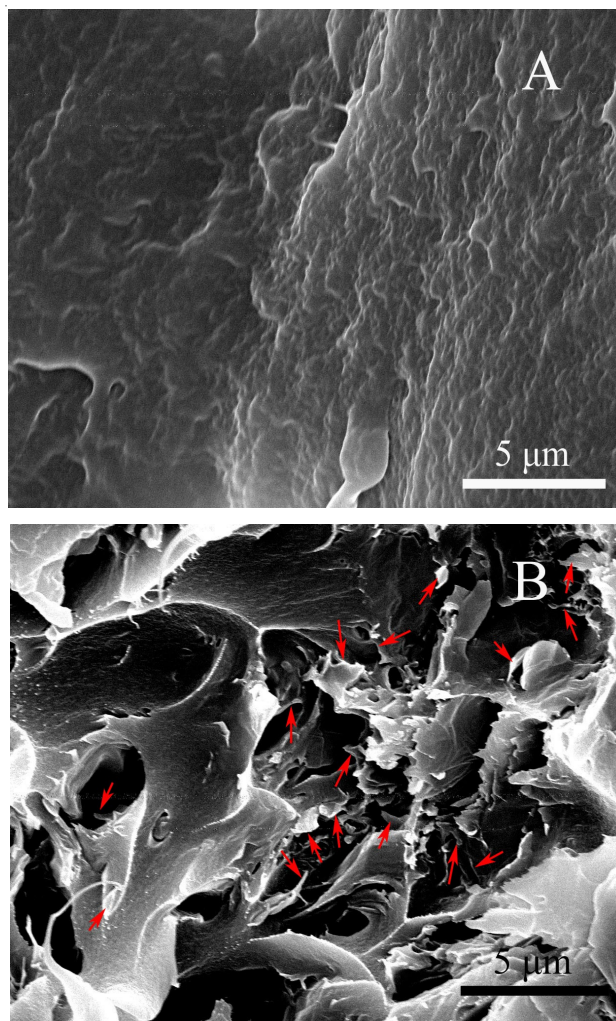


Fig. 5. SEM images of fracture surface of (A) pure poly(vinyl alcohol) and 2 % GO/PVA

dispersibility and strong interaction in poly(vinyl alcohol) matrix. The tensile strength of the composite containing 2 wt. % of graphene oxide increased by 52.3 % from 55.1 to 83.9 MPa and the Young's improved modulus by 94.2 % compared with the pure poly(vinyl alcohol) film (1.55GPa). This approach offers a new avenue for the development of high strength structural materials.

ACKNOWLEDGEMENTS

This work was supported by the National Natural Science Foundation of China (No. 21264001, 21004009), Natural Science Foundation of Jiangxi Province (No. 20114BAB213010), Young Scientist Foundation of Jiangxi Province (No. 20133BCB23020) and Foundation of Jiangxi Educational Committee (No. GJJ14471).

REFERENCES

1. S. Stankovich, D.A. Dikin, G.H.B. Dommett, K.M. Kohlhaas, E.J. Zimney, E.A. Stach, R.D. Piner, S.T. Nguyen and R.S. Ruoff, *Nature*, **442**, 282 (2006).
2. C. Lee, X. Wei, J.W. Kysar and J. Hone, *Science*, **321**, 385 (2008).
3. X. Du, I. Skachko, A. Barker and E.Y. Andrei, *Nat. Nanotechnol.*, **3**, 491 (2008).

4. H. Kim, A.A. Abdala and C.W. Macosko, *Macromolecules*, **43**, 6515 (2010).
5. V. Mittal, *Macromol. Mater. Eng.*, **299**, 906 (2014).
6. H.C. Schniepp, K.N. Kudin, J. Li, R.K. Prud'homme, R. Car, D.A. Saville and I.A. Aksay, *ACS Nano*, **2**, 2577 (2008).
7. H. Schniepp, J. Li, M. McAllister, H. Sai, M. Herrera-Alonso, D.H. Adamson, R.K. Prud'homme, R. Car, D.A. Saville and I.A. Aksay, *J. Phys. Chem. C*, **110**, 8535 (2006).
8. H. Kim, Y. Miura and C.W. Macosko, *Chem. Mater.*, **22**, 3441 (2010).
9. W.H. Lee, J. Park, Y. Kim, K.S. Kim, B.H. Hong and K. Cho, *Adv. Mater.*, **23**, 3460 (2011).
10. H. Wang, L.-F. Cui, Y. Yang, H. Sanchez Casalongue, J.T. Robinson, Y. Liang, Y. Cui and H. Dai, *J. Am. Chem. Soc.*, **132**, 13978 (2010).
11. X.M. Sun, Z. Liu, K. Welscher, J.T. Robinson, A. Goodwin, S. Zaric and H.J. Dai, *Nano Res.*, **1**, 203 (2008).
12. Z. Liu, J.T. Robinson, X.M. Sun and H.J. Dai, *J. Am. Chem. Soc.*, **130**, 10876 (2008).
13. C.H. Lu, H.H. Yang, C.L. Zhu, X. Chen and G.N. Chen, *Angew. Chem. Int. Ed.*, **48**, 4785 (2009).
14. X.-C. Dong, H. Xu, X.-W. Wang, Y.-X. Huang, M.B. Chan-Park, H. Zhang, L.-H. Wang, W. Huang and P. Chen, *ACS Nano*, **6**, 3206 (2012).
15. S. Chen, J. Zhu, X. Wu, Q. Han and X. Wang, *ACS Nano*, **4**, 2822 (2010).
16. V. Chandra, J. Park, Y. Chun, J.W. Lee, I.C. Hwang and K.S. Kim, *ACS Nano*, **4**, 3979 (2010).
17. N.L. Yang, J. Zhai, D. Wang, Y.S. Chen and L. Jiang, *ACS Nano*, **4**, 887 (2010).
18. S. Wang, D. Yu, L. Dai, D.W. Chang and J.-B. Baek, *ACS Nano*, **5**, 6202 (2011).
19. G.M. Scheuermann, L. Rumi, P. Steurer, W. Bannwarth and R. Mulhaupt, *J. Am. Chem. Soc.*, **131**, 8262 (2009).
20. S. Stankovich, D.A. Dikin, G.H.B. Dommett, K.M. Kohlhaas, E.J. Zimney, E.A. Stach, R.D. Piner, S.B.T. Nguyen and R.S. Ruoff, *Nature*, **442**, 282 (2006).
21. O.K. Park, J.Y. Hwang, M. Goh, J.H. Lee, B.C. Ku and N.H. You, *Macromol.*, **46**, 3505 (2013).
22. H.X. Tang, G.J. Ehlert, Y.R. Lin and H.A. Sodano, *Nano Lett.*, **12**, 84 (2012).
23. N. Wu, X.L. She, D.J. Yang, X.F. Wu, F.B. Su and Y.F. Chen, *J. Mater. Chem.*, **22**, 17254 (2012).
24. C.L. Bao, Y.Q. Guo, L. Song and Y. Hu, *J. Mater. Chem.*, **21**, 13942 (2011).
25. T. Ramanathan, A.A. Abdala, S. Stankovich, D.A. Dikin, M. Herrera-Alonso, R.D. Piner, D.H. Adamson, H.C. Schniepp, X. Chen, R.S. Ruoff, S.T. Nguyen, I.A. Aksay, R.K. Prud'homme and L.C. Brinson, *Nat. Nanotechnol.*, **3**, 327 (2008).
26. H. Bai, C. Li, X.L. Wang and G.Q. Shi, *Chem. Commun.*, **46**, 2376 (2010).
27. C.C. Yang, S.J. Chiu, W.C. Chien and S.S. Chiu, *J. Power Sources*, **195**, 2212 (2010).
28. L.Z. Zhang, Y.Y. Wang, C.L. Wang and H. Xiang, *J. Membr. Sci.*, **308**, 198 (2008).
29. J.H. Yeun, G.S. Bang, B.J. Park, S.K. Ham and J.H. Chang, *J. Appl. Polym. Sci.*, **101**, 591 (2006).
30. R. Mukherjee, G.K. Patil and A. Sharma, *Ind. Eng. Chem. Res.*, **48**, 8812 (2009).
31. W.S. Hummers Jr. and R.E. Offeman, *J. Am. Chem. Soc.*, **80**, 1339 (1958).
32. Y. Qian, C.Y. Wang and Z.-G. Le, *Appl. Surf. Sci.*, **257**, 10758 (2011).
33. S. Stankovich, D.A. Dikin, R.D. Piner, K.A. Kohlhaas, A. Kleinhammes, Y. Jia, Y. Wu, S.T. Nguyen and R.S. Ruoff, *Carbon*, **45**, 1558 (2007).